



UROP Report

Epitaxial growth of magnetic kagome metals and transport property measurement

Author: Ce Zheng

Supervisor: Berthold Jäck

CONTENTS

Abstract	ii
1 Introduction	1
2 Research Content	2
2.1 Kagome Metal	2
2.2 Molecular Beam Expitaxy	3
2.2.1 Overview of MBE	3
2.2.2 Effusion cells	3
2.2.3 RHEED	4
2.3 Material growth process with MBE	5
2.3.1 Process of material growth	5
2.3.2 Process of using RHEED	6
2.4 Property Measurement with PPMS	7
2.4.1 Transport Property in solid state physics	7
2.4.2 PPMS and Process for the measurement	8
2.4.3 Data analysis	9
3 Conclusion and Improvement	11
3.1 Conclusion	11
3.2 Improvement	11
3.2.1 Real-time plotting	11
3.2.2 Automatic shutter for MBE	11
References	12
Acknowledgements	14
Appendix A	15

ABSTRACT

In this paper, we focus on the properties, preparation and characterisation of Kagome metal, a new type of metallic material, which is named after its honeycomb lattice structure. The lattice structure of Kagome metal has very specific electronic properties, and therefore exhibits a wide range of physical properties, which are The lattice structure of Kagome metal has very special electronic properties and therefore exhibits a wide range of physical properties.

Generally speaking, there are many methods used to prepare and characterise Kagome metal. In this paper, we focus on the preparation of Kagome metal using the molecular epitaxial beam technique and use a PPMS device to investigate the material properties and to obtain relevant physical conclusions.

Keyword: Kagome metal, Transport property, MBE, Hall effect

1 INTRODUCTION

Kagome metal is a newly discovered material in today's materials science and physics. First discovered in 2011[1], the material has been the focus of research because of its special lattice structure and magnetic properties. The lattice structure of kagome metal is characterised by very specific electronic properties, such as topological insulators and quantum spin liquids. In this experiment, we used FeSn as the research object. Due to the special positional arrangement of Fe and Sn, a kagome structure is formed, which makes its properties change. We carried out a profound study on its key properties such as the special characteristics, Hall effect, transport properties and so on.

Throughout the experiment, we need to carry out a lot of preliminary work. First of all, we need to prepare the Kagome metal, which can be divided into the chemical method of direct metal ion coordination and the high-temperature melting alloy preparation method. We chose the latter, using molecular epitaxial beam technology to fuse Fe and Sn in a vacuum after heating to ultra-high temperatures to form the kagome metal. Throughout the process, we chose to simultaneously use RHEED for observation of the state.[2]

After the successful preparation of kagome metal, we can choose to use XRD technique etc. for property analysis. We finally chose to use the physical properties measurement system (PPMS) to test the transport properties. The anisotropic nature of the kagome metal is analysed by varying the parameters such as the angle of current injection, temperature, magnetic field strength, etc. to study the resistive properties and hence the physical properties. Theoretical and computational analyses are also performed, such as energy band structure analysis using the DFT method.

2 RESEARCH CONTENT

2.1 Kagome Metal

Discovered in 2011 by a team of researchers at the Massachusetts Institute of Technology (MIT), Kagome Metal is named after the unique arrangement of atoms that form a lattice resembling the caged basket structure that characterised ancient Japan, and which, when viewed under a microscope, is vertically projected to resemble the hexagram symbol. Two (or more) atoms are horizontally spaced to form a neat structure. We often use metals such as Fe, Co, etc. in combination with Sn, Ge, etc. to form planar structures, which are expressed in different chemical expressions due to their different ratios. [3] As presented in Figure 2.1. We can focus on FeSn and Fe₃Sn and we mainly study their properties in two dimensions.[1][4]

There have been many studies on their properties in recent years, starting with their special energy band structure, as shown in Figure 2.2 below, which demonstrates the energy band structure of FeSn, for which scientists have performed DFT calculations. Also the Kagome lattice harbours huge Dirac fermions[5], Berry curvature, band gaps and spin-orbit activity, all of which favour the Hall effect and zero energy loss currents. At the same time, the triangular arrangement configuration of its atoms makes it easier to realise the quantum Hall effect, which in turn leads to the expectation of room-temperature superconductivity.

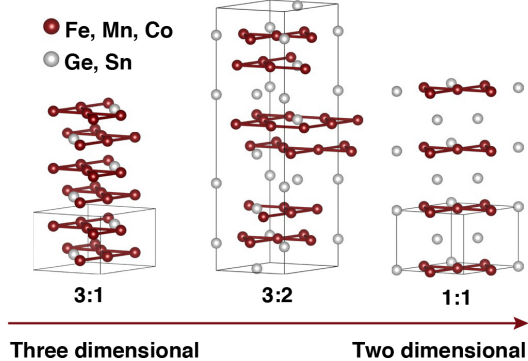


Figure 2.1. FeSn model, kagome metal

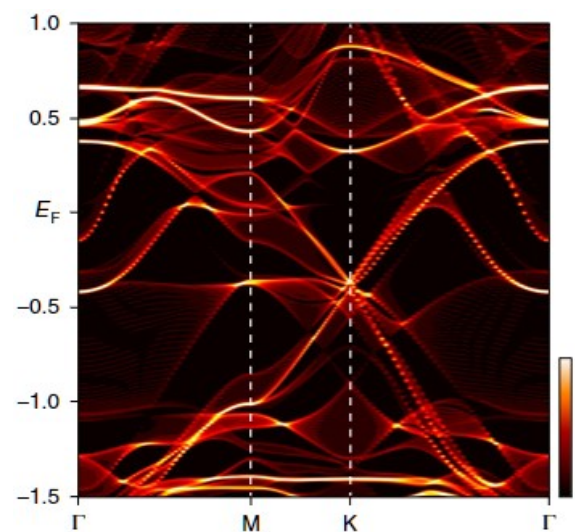


Figure 2.2. The band structure for kagome metal

2.2 Molecular Beam Expitaxy

2.2.1 Overview of MBE

Molecular Beam Epitaxy (MBE) system refers to a kind of epitaxial equipment which is used to epitaxially grow a single crystal thin film along the crystalline axis of the substrate material by one or more beams of thermal atomic beams or molecular beams, which are sprayed onto the surface of the heated substrate at a certain speed under the condition of ultra-high vacuum and adsorbed and migrated along the surface of the substrate.

Its composition is more complex, but the various components are closely coordinated, a clear division of labor. The whole MBE device presents a centrosymmetric figure, in which the middle part is the most core part, used for fixing the substrate, this area is generally a high vacuum environment, the general vacuum degree can be realized for 10^{-10} Torr. [6]the following six similar to the tentacles is the efficiency cell, this is the key to MBE, which is placed in different raw materials, by means of the leakage of This is the key to MBE, in which different raw materials are placed to eject beams of atoms from the raw materials at high temperatures onto the substrate. There is also a transfer device and a monitoring device (RHEED).[2] All these collaborations make up a complete MBE system. They are all shown in Fig2.3 and Fig2.4[7][8]

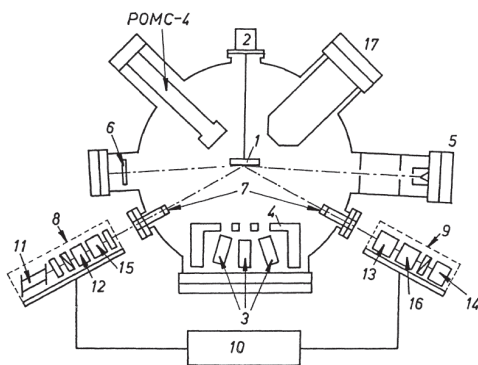


Figure 2.3. The plan view of the front, of which 5 is the electron gun and 6 is the display screen, which constitutes RHEED. The substrate is fixed at 1, and 3 is the effusion cells.

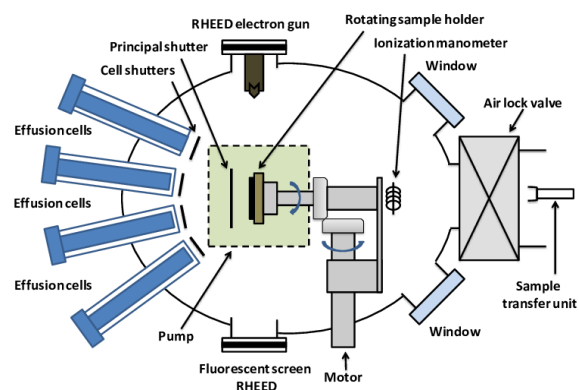


Figure 2.4. Also the front view but it will be more clear

2.2.2 Effusion cells

In particular, we need to hit the atomic beam on the substrate for deposition, which in turn makes the material grow. Then the device is the Effusion cells, which are like a gun

that shoots the atoms out. Typically an MBE will have six of these devices, storing different elements for the growth of the material. The Effusion cells will have a tapering crucible at one end, connected to a thermocouple, which heats the material to thousands of degrees, and a shutter at the other end, which is a switch that controls the release of the material. The thermocouple, by regulating the amount of current and voltage, forms a closed loop in which the coupling of currents occurs, making it generate a huge current, which, by Joule's law, obtains a large temperature. This allows for quantitative temperature control through instrumentation.

As for the shutter, the shutter in this experiment is a normal version, which needs to be manually adjusted in terms of how much air comes out of it.[9] In this experiment, if we need to obtain Fe_3Sn . we have to make sure that the ratio of the release of Fe to Sn is 3:1, which we can obtain thermodynamically by changing the temperature, according to the ideal gas equation of state and Dalton's law of partial pressure:

$$pV = nRT$$

$$p_i = x_i P \quad (i = 1, 2, \dots, n)$$

We need to switch the shutter on and off before the material grows to see the change in temperature and pressure, we can determine the ratio of moles of Fe to Sn released, and thus determine the appropriate pressure and temperature. We can also choose an automated device for shutter control, which is presented later in the improvement.

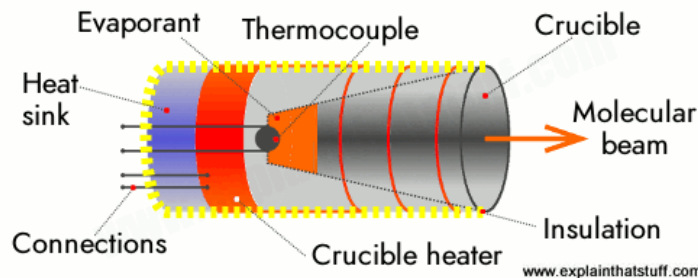


Figure 2.5. This shows the structure for the effusion cell

2.2.3 RHEED

Reflection High-Energy Electron Diffraction (RHEED) is a surface structure characterisation technique commonly used for thin film growth and surface morphology analysis. RHEED uses a high-energy electron beam to irradiate the surface of a sample, and then observes and analyses the reflected electron diffraction patterns. These diffraction patterns provide information about the surface structure of the sample, including lattice constants, crystal orientation, surface flatness, and surface periodicity. As shown in Fig2.6. [10] The main principle is derived from the Bragg diffraction formula $2d \sin \theta = n\lambda$.

Diffraction occurs when an electron beam hits a material sample's surface, creating a diffracted light spectrum that characterises the material's surface morphology. The diffraction pattern's appearance and periodicity reveal the crystal orientation and periodic growth pattern of the thin film. RHEED monitors thin film growth in real-time to provide information on growth rate and surface morphology, with its image showing lattice properties in reciprocal space. The principles of RHEED and XRD are similar, and the Ewald construction technique is used for analysis when the image satisfies the Laue condition. This determines the relationship between the RHEED screen image and lattice morphology.

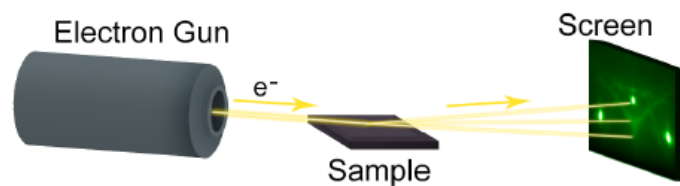


Figure 2.6. A cartoon picture for the RHEED device

2.3 Material growth process with MBE

2.3.1 Process of material growth

- We generally choose Pt for the buffer layer, which we will place on the substrate and pass into the MBE together.
- Connect liquid nitrogen to the device by cooling it down and making an internal vacuum. Connect the RHEED unit after the system has stabilized.
- Adjusting the relevant parameters of the control substrate, a voltage of 1004.0 V and a current of 5.09 mA are generally selected, while ensuring that its pressure is $3e(-10)$ mbar.
- We need to gradually reduce the temperature of the substrate to 140 degrees Celsius with a indicated voltage of 2.215V and current of 2.15A, and an expected electrical heating of 4.8W, totaling about 30 minutes.
- Repeat the same operation to bring the temperature to 80 degrees Celsius while the growth of the material can take place.
- A substrate temperature of about 100 degrees is optimal. After conditioning, we adjusted Fe to 1235°C and Sn to 961°C. The process lasted about 9 hours.

- After the sample is grown, the sample is transferred out through a pipe. The system is then cooled down to restore normal temperature and pressure.

2.3.2 Process of using RHEED

- To monitor the growth and surface condition of a material, RHEEDs are used throughout the growth process. The light source need to be turned on from the beginning of the material growth, and its approximate position is shown.
- To view the picture in real time, an external camera is connected to a computer, which provides a clear image after adjusting the focus and fixing it with a screw.
- With an external remote control, we can adjust the brightness, intensity, and position of the particle beam, and fine-tune the image as the reaction progresses. Real-time data recording provides a clear picture of the material's surface morphology and lattice arrangement.

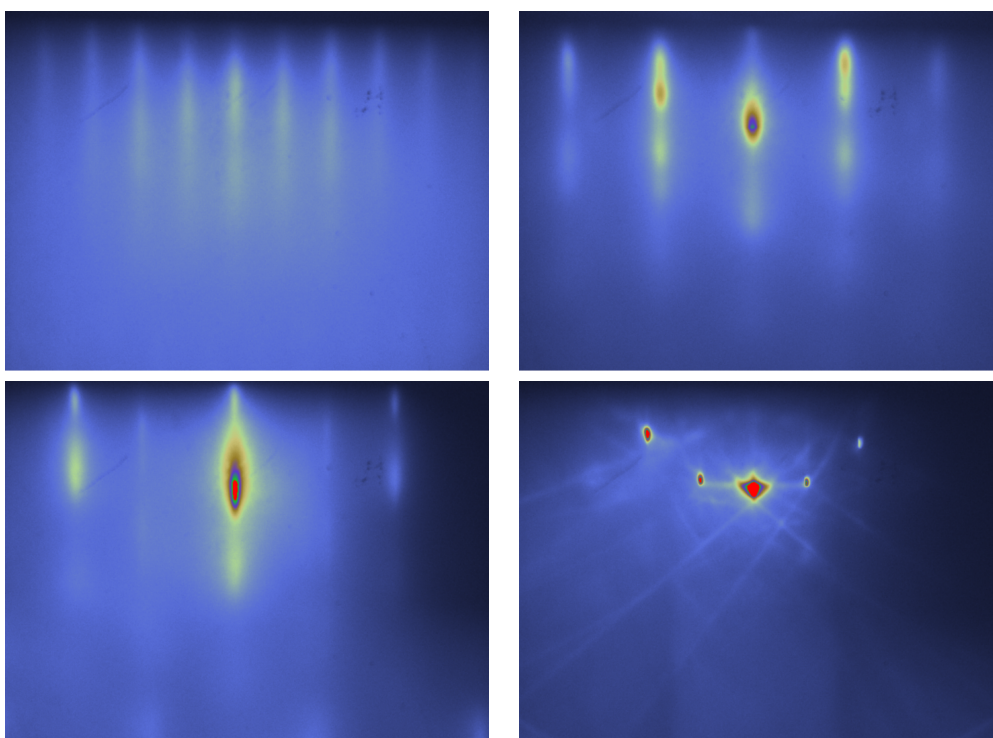


Figure 2.7. This describes the RHEED pattern changing process during the whole sample growth.

2.4 Property Measurement with PPMS

2.4.1 Transport Property in solid state physics

The transport properties of 2D materials refer to the behavior and characteristics of particles, such as electrons, that are transported through the material in the 2D plane. The transport properties of 2D materials are closely related to their electronic and lattice structures, and we can generally find the carrier properties of 2D materials through the measurement of their transport properties. We will also study the properties of Dirac fermions that some electrons have, i.e., zero mass and linear dispersion relations near their Fermi surface, and thus study key factors such as the quantum Hall effect.[11]

We generally start by the conductivity of the material, according to the formula $\sigma = nq\mu_- + pq\mu_+$ where μ_- and μ_+ are the numbers of electrons and holes, respectively. Where n is the carrier density μ is the carrier mobility. We need to focus on the carrier density and carrier mobility in the test of transport properties to summarize the study separately. We can usually obtain the optical system for the carrier density in the conduction band. The expression is as follows.[12]

$$n_0 = N_c \exp\left(-\frac{E_c - E_F}{k_B T}\right)$$

Here, both E_c and E_F are related to the material's own properties, which are strongly affected by the material's composition, defects, and impurities, and they correspond to the conduction-band bottom energy and the Fermi energy level, respectively. However, N_c in Eq. denotes the effective density of states of the conduction band, which is derived from the Boltzmann distribution:

$$N_c = 2 \times \frac{(2\pi m_n k_B T)^{3/2}}{h^3}$$

For carrier mobility, this indicates how easy it is for carriers to migrate through the material, this is usually influenced by impurities and defects and is usually independent of temperature. We generally derive its formula $\mu = \frac{q}{pm}$ from statistical physics.

As for the measurement of its resistivity, we usually choose the four-probe method, which is one of the very common methods used in analyzing the transport properties of materials. In this method, we inject a current with a current density of J , which is bound to excite an electric field of E . Through Ohm's law, we can obtain its expression $\sigma = \frac{J}{E} = \frac{Il}{VA}$ where V is the potential difference between the probes, l is the distance between the probes, and A is the sample surface area. However, for two-dimensional materials, whose thickness is much smaller than the probe spacing, we need to correct the formula, and we get the following formula, where r corresponds to the distance between the probes and t is the material thickness.

$$\rho = \frac{2\pi t V_{23}}{I} / \ln\left(\frac{r_{42} \times r_{13}}{r_{43} \times r_{12}}\right)$$

2.4.2 PPMS and Process for the measurement

PPMS is a vacuum device that uses a controlled magnetic field and temperature to measure the transport properties of a sample. Control the current, temperature, and magnetic field using an automated process using the program and Python software. The main body of PPMS consists of a large tank filled with liquid helium and liquid nitrogen, vacuum equipment, and an external current source and lock-in amplifier. Use the rod to insert the sample into the device and start the measurement after fixing the holder as needed.[13]

In this experiment, we need to study the transport properties of kagome metal FeSn. Due to its anisotropy, we need to vary the angle of the injected current and measure the corresponding horizontal and vertical voltages, i.e., V_{xx} and V_{xy} . (Fig2.8) In turn, we study the resistance and carrier density. However, in this measurement, since we want to study its anisotropic character. We choose different input angles of the current and measure its corresponding voltage values. We divided into twelve equal angles for separate current injection as well as measurement. (Fig2.9)[14]

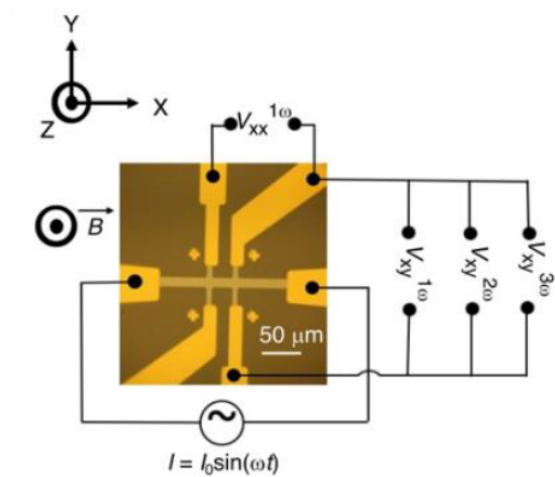


Figure 2.8. The four probe measurement for 2D materials, the I and V are both perpendicular

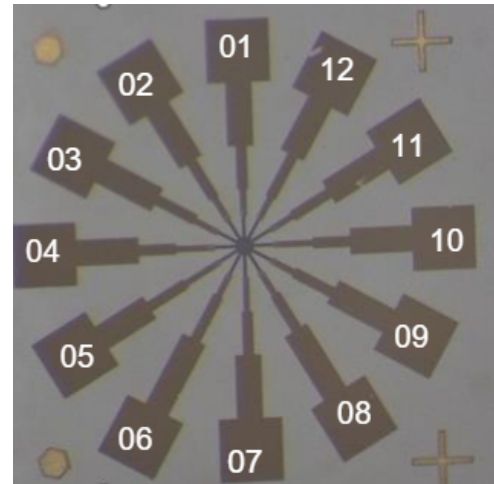


Figure 2.9. The connection model we use in the experiment, 12 probes in total

The whole operation is shown in the flowchart, followed by its detailed process

- Initialize all equipment first, including making sure that the PPMS vacuum environment, current sources, and lock-in amplifiers are intact. Connect the corresponding wires (i.e. connect the current source and the lock-in amplifier to the different ends of the sample) open the python program and the PPMS PC console program and run the program adjusted to the desired measurement range.
- After starting the measurement, we need to keep an eye on the change of the pressure inside the PPMS in real time to keep it safe. python program will automatically collect the corresponding current and voltage values and generate the corresponding csv file.

- We will analyze the csv file plots so that we can get the relationship between resistivity, temperature, and magnetic field in different cases.

2.4.3 Data analysis

Since the measurement process is automated, we will get a csv file dataset. We generally choose different temperatures and analyze their situation separately. We first perform Zero field Hall analysis on it. ZFHA measures the charge distribution on the surface of semiconductor materials under zero magnetic field. This method can determine the carrier concentration and type of semiconductor materials, so we usually select the connection angle first. (deg), draw its image, as shown in Figure 2.10. Next we need to measure, at different temperatures, how the voltage varies with the magnetic field. Repeat the measurement many times to get multiple sets of csv files. We use matlab code to read csv files and plot them. We first get a curve similar to Figure 2.11, which depicts the resistance versus temperature.

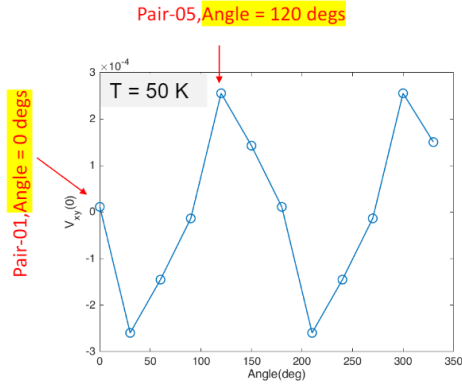


Figure 2.10. ZFHA plot with different degrees

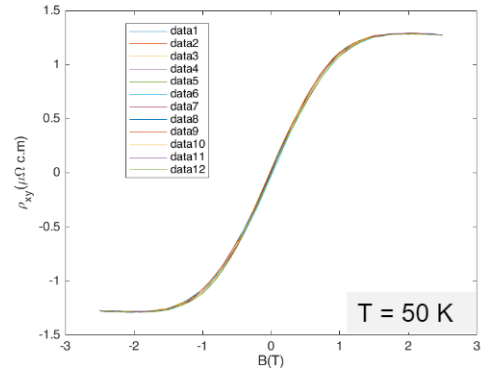
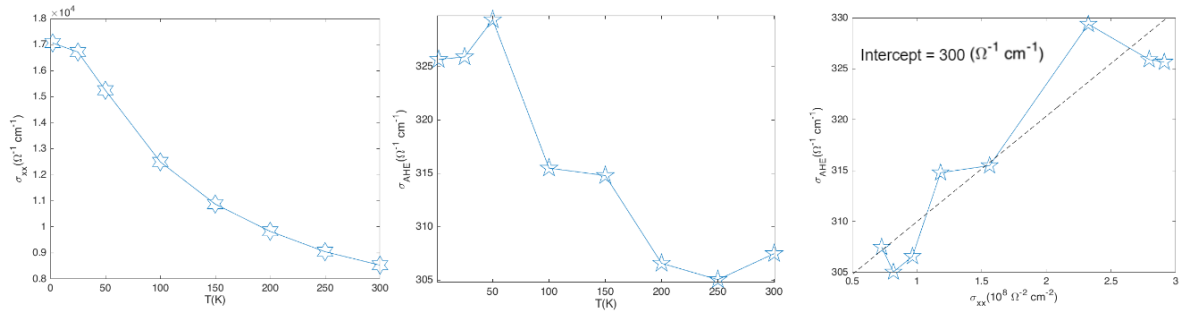


Figure 2.11. example plot of ω - B

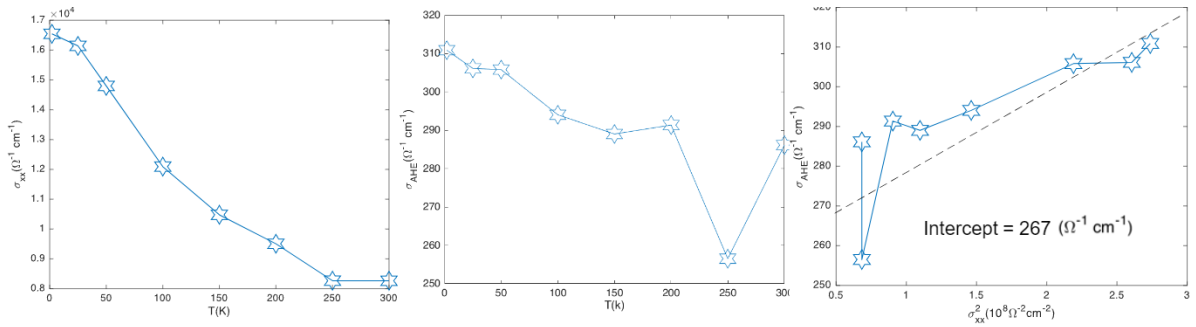
In the specific experiment, we measured the cases of 0° and 120° , we take . For this example, we can get a similar graph of resistivity versus temperature

Next, we will study the relationship between resistivity and carrier density in the case of High field saturation. We will study and measure the resistivity ρ_{xx} and ρ_{xy} in the horizontal and vertical directions. Through the extension method of the four-probe method, we can know that the transverse and longitudinal resistivities are $\sigma_{xx} = \frac{\rho_{xx}}{\rho_{xx}^2 + \rho_{xy}^2}$ and $\sigma_{xy} = \frac{\rho_{xy}}{\rho_{xx}^2 + \rho_{xy}^2}$ respectively. Then for the resistivity research of its Anomalous Hall Effect, we choose the corresponding formula $\sigma_{AHE} = f(\sigma_{xx,0})\sigma_{xx}^2 + \sigma_{xy}^{int}$, For the measurement of the migration rate, we usually choose the formula mentioned in the above section, and then draw the image. We can get the following two figures(Fig 2.12) about the relation between σ_{xy} and σ_{AHE} .

Finally, according to the formula $R_H = \frac{E_y}{J_x \cdot B}$, we find the Hall coefficient and the carrier density when the Hall effect occurs and draw the image. Taking the case of 0° as an example,



(a) Degree = 120°



(b) Degree = 0°

Figure 2.12. relation between σ_{xy} and σ_{AHE}

we have found through image analysis that the Hall coefficient increases with the increase of temperature, and the carrier density is stable in the $10^{-22} - 23$ range, and fluctuates greatly between 150-200K, which means, the carrier type switching from holes to electrons is observed. (Fig2.13 and Fig2.14)

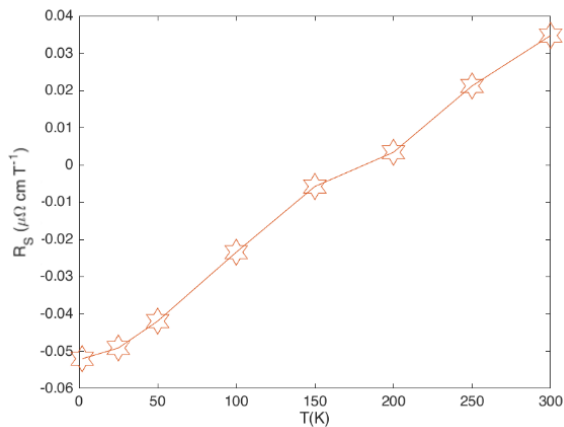


Figure 2.13. Hall coefficient in 0°

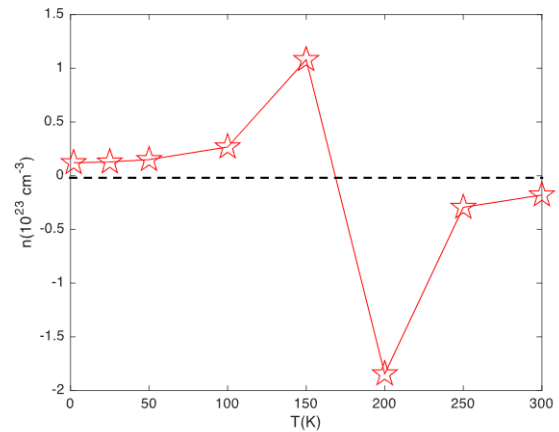


Figure 2.14. Carrier Density in 0°

3 CONCLUSION AND IMPROVEMENT

3.1 Conclusion

This report covers two main parts: growing kagome material (FeSn) using molecular beam epitaxy (MBE) technology and testing its transport properties. In addition, minor tasks were carried out and will be discussed in the following section.

To grow FeSn with MBE, we adjusted the instrument parameters based on RHEED measurements and repeated experiments until we obtained samples with perfect morphology. This will facilitate subsequent material characterization and analysis. Our group is also working on determining the most accurate parameters for growing the material.

For transport property testing using PPMS, we produced multiple sets of images to determine resistivity and carrier density under different conditions. The images clearly exhibit the material's quantum Hall effect and unique transport properties, representing a breakthrough in FeSn research. We also collaborated with other research groups to simulate and establish a more comprehensive system for this material, which may facilitate its future applications in production and daily life.

3.2 Improvement

3.2.1 Real-time plotting

In order to facilitate the measurement of transport properties, operate PPMS and other instruments, and monitor the measured data at the same time, I designed a python program for real-time display, as shown in the code in Appendix A.

3.2.2 Automatic shutter for MBE

We choose ESP-32 single-chip microcomputer as the central control, one end of which is connected to the computer, and the other end is connected to the stepper motor by using PyCharm to run the program. The motor selection is controlled by the computer program, and then the angle and time of the shutter switch are automatically controlled.

REFERENCES

- [1] Mingu Kang, Linda Ye, Shiang Fang, Jhih-Shih You, Abe Levitan, Minyong Han, Jorge I. Facio, Chris Jozwiak, Aaron Bostwick, Eli Rotenberg, Mun K. Chan, Ross D. McDonald, David Graf, Konstantine Kaznatcheev, Elio Vescovo, David C. Bell, Efthimios Kaxiras, Jeroen van den Brink, Manuel Richter, Madhav Prasad Ghimire, Joseph G. Checkelsky, and Riccardo Comin. Dirac fermions and flat bands in the ideal kagome metal fesn. *Nature Materials*, 19(2):163–169, Feb 2020.
- [2] Tsunenori Sakamoto. Rheed oscillations in MBE and their applications to precisely controlled crystal growth. In *Physics, Fabrication, and Applications of Multilayered Structures*, pages 93–110. Springer US, 1988.
- [3] Linda Ye, Mingu Kang, Junwei Liu, Felix von Cube, Christina R. Wicker, Takehito Suzuki, Chris Jozwiak, Aaron Bostwick, Eli Rotenberg, David C. Bell, Liang Fu, Riccardo Comin, and Joseph G. Checkelsky. Massive dirac fermions in a ferromagnetic kagome metal. *Nature*, 555(7698):638–642, Mar 2018.
- [4] Motohiko Ezawa. Higher-order topological insulators and semimetals on the breathing kagome and pyrochlore lattices. *Phys. Rev. Lett.*, 120:026801, Jan 2018.
- [5] Seung-Hwan Do, Koji Kaneko, Ryoichi Kajimoto, Kazuya Kamazawa, Matthew B. Stone, Jiao Y. Y. Lin, Shinichi Itoh, Takatsugu Masuda, German D. Samolyuk, Elbio Dagotto, William R. Meier, Brian C. Sales, Hu Miao, and Andrew D. Christianson. Damped dirac magnon in the metallic kagome antiferromagnet FeSn. *Physical Review B*, 105(18), May 2022.
- [6] Deshun Hong, Changjiang Liu, Haw-Wen Hsiao, Dafei Jin, John E. Pearson, Jian-Min Zuo, and Anand Bhattacharya. Molecular beam epitaxy of the magnetic kagome metal FeSn on LaAlO₃ (111). *AIP Advances*, 10(10), October 2020.
- [7] Helmut Sitter Marian A. Herman. Molecular beam epitaxy fundamentals and current status. Jan 1996.
- [8] Shuyu Cheng, Binbin Wang, Igor Lyalin, Núria Bagués, Alexander J. Bishop, David W. McComb, and Roland K. Kawakami. Atomic layer epitaxy of kagome magnet $\text{FeSn}_3/\text{SnS}_2/\text{Sn}$ and Sn -modulated heterostructures. *APL Materials*, 10(6):061112, June 2022.

- [9] Shin ichiro Gozu, Teruo Mozume, Haruhiko Kuwatsuka, and Hiroshi Ishikawa. Effects of shutter transients in molecular beam epitaxy. *Nanoscale Research Letters*, 7(1), November 2012.
- [10] Nassim Derriche, Simon Godin, Rysa Greenwood, Alejandro Mercado, and Ashley Nicole Warner. Reflection high-energy electron diffraction. 2019.
- [11] Ming Zhang, Ekkes Brück, Frank R. de Boer, and Guangheng Wu. Electronic structure, magnetism, and transport properties of the heusler alloy Fe_2CrAl . *Journal of Magnetism and Magnetic Materials*, 283(2-3):409–414, December 2004.
- [12] Rongqing Hui and Maurice O'Sullivan. Characterization of optical devices. In *Fiber Optic Measurement Techniques*, pages 259–363. Elsevier, 2009.
- [13] Kohei Fujiwara, Yasuyuki Kato, Takeshi Seki, Kentaro Nomura, Koki Takanashi, Yukitoshi Motome, and Atsushi Tsukazaki. Tuning scalar spin chirality in ultrathin films of the kagome-lattice ferromagnet Fe_3Sn . *Communications Materials*, 2(1), November 2021.
- [14] Soumya Sankar, Ruizi Liu, Xue-Jian Gao, Qi-Fang Li, Caiyun Chen, Cheng-Ping Zhang, Jiangchang Zheng, Yi-Hsin Lin, Kun Qian, Ruo-Peng Yu, Xu Zhang, Zi Yang Meng, Kam Tuen Law, Qiming Shao, and Berthold Jäck. Observation of the berry curvature quadrupole induced nonlinear anomalous hall effect at room temperature, 2023.

ACKNOWLEDGEMENTS

In this scientific research project, I would like to thank my supervisor Berthold Jaeck for his support and careful teaching throughout the experiment. At the same time, I would like to thank Mr. Soumya Sankar for helping and teaching me to use MBE and RHEED together. I would also like to thank Mr. Soumya Sankar and Ms. Yuqi Qin for cooperating with the author in the project of transport property measurement. I would also like to thank Mr. Yizhou Wei for designing the improved shutter. Finally, I would also like to thank the UROP committee and HSEO for the experimental safety training and scientific research training for the author.

APPENDIX A

This is the python code for real time plotting.

```
1
2 import numpy as np
3 import time
4 #import tkinter.filedialog
5 #import tkinter as tk
6 import pyvisa as py
7 #import pandas as pd
8 #from tkinter import ttk
9 #import threading
10 #import time
11 from labdrivers.quantumdesign import Ppms
12 import matplotlib
13 matplotlib.use('Qt5Agg')
14 '''
15 we use matplotlib to generate a new window for animation plotting
16 '''
17
18 import matplotlib.pyplot as plt
19 import numpy as np
20 #k2636 = keithley_2636B("USB0::0x05E6::0x2636::4443485::INSTR")
21 max_field = -40000 # the maximum magnetic field
22 linear = True # field changes linearly or in a square root
23 direction = True # False for singla sweep and True for double sweep
24 num_field = 41 # the field point of field
25 #Temp = [100] # the temperature
26 delay = 5 #wait after wait condition achieved in seconds
27 timeout = 600 #wait to achieve wait condition in seconds
28 error = 100
29 Rate_B = 80 #0e/s
30 Rate_T = 30
31 field = np.linspace(0, 1, num_field)
32 lists = {}
33
34 for i in range(1, 2):
35     for j in range(1, 4):
36
37         list_name = 'list{}.{}'.format(i, j)
38         lists[list_name] = []
39 '''
```

```

40 we create a 1*3 lists, because we only choose 1 temprature and 3
    parameters(B filed, Vxx, Vxy)
41 '''
42 #print(lists.keys())
43 try:
44     lock_in_1 = 'GPIB0::12::INSTR'
45     #lock_in_2 = 'GPIB0::10::INSTR'
46     #lock_in_3 = 'GPIB0::13::INSTR'
47     #lock_in_4 = 'GPIB0::08::INSTR'
48     #lock_in_5 = 'GPIB0::12::INSTR'
49     #lock_in_6 = 'GPIB0::16::INSTR'
50     address_6221 = 'GPIB0::13::INSTR'
51     rm = py.ResourceManager()
52     equ_6221 = rm.open_resource(address_6221, write_termination = '\n', read_termination = '\n')
53     harmonic_1 = rm.open_resource(lock_in_1, write_termination = '\n', read_termination = '\n')
54     # harmonic_2 = rm.open_resource(lock_in_2, write_termination = '\n', read_termination = '\n')
55     time.sleep(0.1)
56     # harmonic_3 = rm.open_resource(lock_in_3, write_termination = '\n', read_termination = '\n')
57     #harmonic_4 = rm.open_resource(lock_in_4, write_termination = '\n', read_termination = '\n')
58     #time.sleep(0.1)
59     #harmonic_5 = rm.open_resource(lock_in_5, write_termination = '\n', read_termination = '\n')
60     #harmonic_6 = rm.open_resource(lock_in_6, write_termination = '\n', read_termination = '\n')
61     #time.sleep(0.1)
62 except :
63     print("GPBI hardware missing")
64     while 1:
65         time.sleep(0.1)
66 if linear:
67     temp_field = -max_field*field[::-1]
68     field = np.append(temp_field[:-1], max_field*field)
69 else:
70     temp_field = [- i*i*max_field for i in field[::-1]]
71     field = np.append(temp_field[:-1], [i*i*max_field for i in field])
72 if direction:
73     pass
74 else:
75     tem_field = field[::-1]
76     field = np.append(field, tem_field)
77 sample_field = field.tolist()

```

```

78 print(sample_field)
79 #angle = [87]
80 #field_m = []
81 #field_p = []
82 #for i in range(1,31):
83     # field_p.append(i*1/30)
84     # field_m.insert(0,-i*1/30)
85 #for i in range(1,21):
86     # field_p.append(i*0.2+1)
87     # field_m.insert(0,-i*0.2-1)
88 #real_field = field_m + [0] + field_p
89 #field_1 = real_field[::-1] + real_field
90 #time.sleep(3600)
91 temperature_list = [300]
92 i = -1
93 PPMS = Ppms('143.89.191.230')
94 for setting_tem in temperature_list:
95     file_name = 'Fe3Sn_DEV_02_2.1mA_19.375HZ' + str(setting_tem) + '
300K_Hall_Pair12'
96     f = open(file_name + '.csv','a+')
97     f.write("B,Vxx_1_X,Vxx_1_Y,Vyx_1_X,Vyx_1_Y,Vyx_3_X,Vyx_3_Y,T_B\
n")
98     T_B = PPMS.getTemperature()
99     #PPMS.setTemperature(setting_tem, 20)
100    #PPMS.waitForTemperature(5, 600)
101    Cur_Tem = T_B[1]
102    print(Cur_Tem)
103    equ_6221.write('SOUR:WAVE:AMPL 2.1e-3')
104    #equ_6221.write('SOUR:WAVE:FREQ 19.357')
105    equ_6221.write('SOUR:WAVE:RANG BEST')
106    time.sleep(0.1)
107    equ_6221.write('SOUR:WAVE:ARM')
108    equ_6221.write('SOUR:WAVE:INIT')
109    time.sleep(10)
110    for target_field in sample_field:
111        # MSS.set_field(target_field, 1)
112        time.sleep(15)
113        # F_B = MSS.get_SMS_ramping()8
114        # while F_B:
115            # time.sleep(1)
116            # F_B = MSS.get_SMS_ramping()
117        PPMS.setField(target_field, Rate_B)
118        errorcode = 1
119        while errorcode != 0:
120            #print('Finish setField')
121            time.sleep(10)
122            print('bad loop')

```

```

123         real_field = PPMS.getField()[1]#Read the real data
instead of the set point
124         if abs(real_field-target_field)< error:
125             errorcode = 0
126         else:
127             pass
128     #print('Finish getfield')
129     Cur_field = PPMS.getField()
130     print('Current Field = %f Gauss' %(Cur_field[1]))
131     time.sleep(5)
132     for j in range(1,3):
133         li_1_X = float(harmonic_1.query('OUTP? 1'))
134         time.sleep(0.1)
135         #li_2_X = float(harmonic_2.query('OUTP? 1'))
136         #time.sleep(0.1)
137         #li_3_X = float(harmonic_3.query('OUTP? 1'))
138         #time.sleep(0.1)
139         #li_4_X = float(harmonic_4.query('OUTP? 1'))
140         #time.sleep(0.1)
141     for j in range(1,3):
142         li_1_Y = float(harmonic_1.query('OUTP? 2'))
143         time.sleep(0.1)
144         #li_2_Y = float(harmonic_2.query('OUTP? 2'))
145         #time.sleep(0.1)
146         #li_3_Y = float(harmonic_3.query('OUTP? 2'))
147         #time.sleep(0.1)
148         # li_4_Y = float(harmonic_4.query('OUTP? 2'))
149         # time.sleep(0.1)
150     #time.sleep(3600)
151     T_B = PPMS.getTemperature()
152     Cur_field = PPMS.getField()
153     time.sleep(0.1)
154     a="list"+str(setting_tem)+".1"
155     b="list"+str(setting_tem)+".2"
156     c="list"+str(setting_tem)+".3"
157     lists[a].append(Cur_field[1])
158     lists[b].append(li_1_X)
159     lists[c].append(li_1_Y)
160     #print(str(keithley_2182_read_xy) + ',' +str(
keithley_2182_read_xx) + ',' +str(B_digital[0]) + ',' \
161         # +str(B_analog[0])+', ' + str(T_A[0]) + ',' + str(
T_B[0]) + '\n')
162     f.write(str(Cur_field[1])+ ', ' + str(li_1_X) + ',' +str(
li_1_Y)+'\n')
163     # time.sleep(3600)
164     # f.write(str(B_analog[0])+', ' + str(li_1_X) + ',' +str(li_1_Y
) + ', ' \

```

```

165     # +str(li_2_X) + ',' + str(li_2_Y) + ',' + str(li_3_X) + ',' + str(
li_3_Y) + ',' \
166     # +str(B_digital[0]) + ',' + str(T_A[0]) + ',' + str(T_B[0])
+ '\n')
167     f.flush()
168
169     time.sleep(3)
170     fig, ax = plt.subplots()
171     ax.cla()
172     ax.scatter(lists["list1.1"], lists['list1.2'])
173     ax.plot(lists["list1.1"], lists['list1.2'])
174     ax.legend()
175     plt.pause(0.1)
176     '''
177     for i in range(1,2):
178         ax.cla()
179         ax.scatter(lists['list{}.1'.format(i)], lists['list
{}.2'.format(i)])
180         ax.legend()
181         plt.pause(0.1)
182     '''
183
184     equ_6221.write('SOUR:WAVE:ABOR')
185     f.close()
186     #i = i + 1
187     #MSS.set_temperature(295, 10)
188     #MSS.set_field(0, 2)

```